Generating quantizing pseudomagnetic fields by bending graphene ribbons

F. Guinea[1], A. K. Geim[2], M. I. Katsnelson[3], K. S. Novoselov[4]

[1] *Instituto de Ciencia de Materiales de Madrid, CSIC,*
Sor Juana Inés de la Cruz 3 E28049 Madrid, Spain

[2] *Centre for Mesoscience and Nanotechnology, University of Manchester, Manchester M13 9PL, United Kingdom*

[3] *Institute for Molecules and Materials, Radboud University of Nijmegen,*
Heyendaalseweg 135, NL-6525 AJ, Nijmegen, The Netherlands

[4] *School of Physics & Astronomy, University of Manchester, Manchester, M13 9PL, United Kingdom*

We analyze the mechanical deformations that are required to create uniform pseudomagnetic fields in graphene. It is shown that, if a ribbon is bent in-plane into a circular arc, this can lead to fields exceeding 10T, which is sufficient for the observation of pseudo-Landau quantization. The arc geometry is simpler than those suggested previously and, in our opinion, has much better chances to be realized experimentally soon. The effects of a scalar potential induced by dilatation in this geometry is shown to be negligible.

Graphene exhibits a number of unique features not found in conventional metals and insulators.[1,2] Among them is the possibility to stretch graphene elastically by more than 15%[3], and to control in different ways the induced strains[4,5,6,7,8,9,10,11]. This offers a prospect of tuning electronic characteristics of graphene devices not only by external electric field but also by mechanical strain[2,12], a possibility being extensively discussed theoretically[12,13,14,15,16,17,18,19,20,21]. In particular, the presence of two valleys at the opposite corners of graphene's Brillouin zone implies that long wavelength lattice deformations induce an effective gauge field acting on the electrons and holes, which has the opposite sign for the two valleys.[1,22,23] This yields an enticing possibility of creating such gauge fields that would mimic a uniform magnetic field B and, consequently, generate energy gaps in the electronic spectrum and lead to a zero-B analogue of the quantum Hall effect.[24] Both isotropic and uniaxial strains result[12,24] in zero pseudomagnetic field B_S but as shown recently[24] deformations with a triangular symmetry can lead to strong uniform B_S. Moreover, the strained-induced pseudomagnetic field can easily reach quantizing values, exceeding 10T in submicron devices for deformations less than 10%.[24]

Unfortunately, all the geometries of applied strain, which were suggested previously,[24] are rather difficult to realize experimentally. In this Communication, we report an alternative strain configuration that does not require a complex triangular symmetry and, in fact, is a straightforward extension of the geometry typically used in experimental studies of strained devices[8,10,11]. We have found that simple in-plane bending of graphene ribbons (see Fig. 1) should lead to strong practically uniform B_S. We believe that this finding can speed up the observation of the pseudomagnetic quantum Hall effect and related phenomena.

First, let us complete the analysis of Ref.24 by classifying the strain distributions that are compatible with equilibrium elasticity and lead to a uniform pseudomagnetic field.

We will use the coordinates that are fixed with respect to graphene's honeycomb lattice in such a way that the
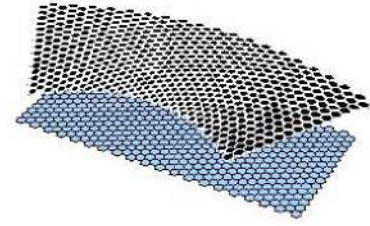

FIG. 1: (Color online). Sketch of the suggested bending geometry that would generate a uniform pseudomagnetic field and open band gaps in graphene's electronic spectrum. The graphene rectangle (lower image) is bent into a circular arc (upper).

x axis corresponds to a zigzag direction. In this case, the gauge field A acting on charge carriers in graphene can be written as[22,23]

$$A_x = \pm c\frac{\beta}{a}\left(u_{xx} - u_{yy}\right)$$
$$A_y = \mp 2c\frac{\beta}{a}u_{xy} \tag{1}$$

where $\beta = -\partial \log(t)/\partial \log(a)$, where $t \approx 3\text{eV}$ is the electron hopping between p_z orbitals located at nearest neighbor atoms, $a \approx 1.4\text{Å}$ is the distance between them, c is a numerical constant that depends on the details of atomic displacements within the lattice unit cell, and u_{ij} is the strain tensor. The two signs correspond to the two valleys, K and K' in the Brillouin zone of graphene.

In two dimensional elasticity problems, it is convenient to study the stress tensor, $\sigma_{ij} = \partial \mathcal{F}/\partial u_{ij}$, where $\mathcal{F}$ is the elastic energy[25]. The gauge field can be written in terms of the stress tensor as

$$A_x = \pm c\frac{\beta}{2a\mu}\left(\sigma_{xx} - \sigma_{yy}\right)$$
$$A_y = \mp c\frac{\beta}{\mu a}\sigma_{xy} \tag{2}$$

where μ is a Lamé coefficient. Furthermore, possible stress distributions that describe two dimensional elastic systems in equilibrium can be written in terms of complex variables $z = x + iy$ and $\bar{z} = x - iy$ as[25]

$$\sigma_{xx} = \frac{\partial^2 f(z, \bar{z})}{\partial y^2}$$
$$\sigma_{yy} = \frac{\partial^2 f(z, \bar{z})}{\partial x^2}$$
$$\sigma_{xy} = -\frac{\partial^2 f(z, \bar{z})}{\partial x \partial y} \quad (3)$$

Here $f(z, \bar{z})$ is either the real or the imaginary part of a function

$$\mathcal{F}(z, \bar{z}) = \mathcal{F}_1(z) + \bar{z}\mathcal{F}_2(z) \quad (4)$$

where $\mathcal{F}_1(z)$ and $\mathcal{F}_2(z)$ are analytic functions. For the case of pure shear deformations considered in Ref.24 $\mathcal{F}_2 = 0$ but here we will not restrict ourselves by this limitation. Since both stress and A are given by the second derivatives of $\mathcal{F}$, whereas B_S is given by the first derivatives of A, a uniform B_S necessitates $\mathcal{F}$ to have a cubic dependence on the coordinates. Such a function must have the following structure:

$$\mathcal{F}(x, y) = c_1(x + iy)^3 + c_2(x - iy)(x + iy)^2 \quad (5)$$

where c_1 and c_2 are arbitrary constants. Separating the real and imaginary part of equation (6), we find four possible functions that result in uniform B_S

$$f(x, y) \propto \begin{cases} x^3 - 3xy^2 \\ x^3 + xy^2 \\ 3x^2y - y^3 \\ x^2y + y^3 \end{cases} \quad (6)$$

The second pair of the solutions is equivalent to the first one by swapping the axes. For the lattice orientation used in Eq. (1), the first pair leads to a gauge field such that $A_x \propto x$ and $A_y \propto y$ and, accordingly, B_S is zero. Hence, the stress distributions that give rise to a uniform pseudomagnetic field can be expressed in terms of a superposition of the functions in lines 3 and 4. The strain configuration found in ref.24 involves only the 3rd function $f(x, y) \propto 3x^2y - y^3$, which leads to a unique solution for the shape of graphene flake where such distribution of stresses can be created by normal forces only. Unfortunately, this solution is not easy to realize experimentally. The use of both 3rd and 4th functions offers further possibilities.

In the following, we consider the deformations required to create a uniform B_S inside a rectangular graphene crystal, of width W and length L, with normal forces applied at the left and right boundaries as sketched in Figure 2. The non-deformed crystal fills the region $-L/2 \leq x \leq L/2, -W/2 \leq y \leq W/2$. Let us write the forces at the right and left boundaries $x = \pm L/2$ as

$$F_x^{R,L} = f_0^{R,L} + f_1^{R,L}y$$
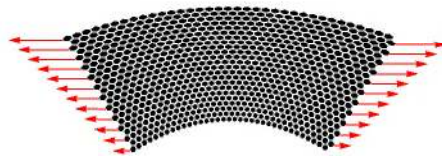$$F_y^{R,D} = 0 \quad (7)$$

FIG. 2: (Color online). Stretching geometry leading to a uniform pseudomagnetic field inside a rectangular graphene sample. Normal forces are applied at two opposite boundaries and their magnitude is indicated by the length of the plotted arrows.

The condition of zero total force and zero total torque requires $f_0^R = -f_0^L = f_0$ and $f_1^R = -f_1^L = f_1$ where f_0 and f_1 are constants. The absence of forces at the upper and lower edges implies that $\sigma_{yy} = \sigma_{xy} = 0$ there. At the right and left edges, we have

$$\sigma_{xx} = \sigma_0 \left(y + \frac{f_0}{f_1} \right)$$
$$\sigma_{xy} = 0 \quad (8)$$

where σ_0 is a constant that depends on applied forces. A stress distribution within the crystal, which is compatible with these boundary conditions, is generated by a function $f(y) = C[y^3/3 + (f_0/f_1)(y^2/2)]$. This function can be considered as a superposition of solutions 3 and 4 of Eq. (6), which leads to a uniform B_S, and a constant term that describes a uniaxial strain and does not give rise to an additional pseudomagnetic field. The latter term ensures that the lattice is stretched everywhere, there is no possibility for out of plane deformations. Inside the rectangular crystal, σ_{xx} depends only on y in the manner described by eq. (8), and $\sigma_{yy} = \sigma_{xy} = 0$. From this stress distribution, we find the lattice distortions

$$u_x = u_0 \left(2xy + \frac{f_0}{f_1}x \right)$$
$$u_y = u_0 \left[-x^2 - \frac{\lambda}{\lambda + 4\mu} \left(y^2 + \frac{f_0}{f_1}y \right) \right] \quad (9)$$

where u_0 is a constant that defines the maximum stress. These displacements lead to the curved shape shown in Fig. 2, which was drawn using the reported[26] Lamé coefficients of graphene, $\lambda \approx 3.3$eV Å^{-2} and $\mu \approx 9.4$eV Å^{-2}. The maximum strain occurs at the top and bottom boundaries and can be estimated as $\bar{u}_{max} \approx u_0(W + f_0/f_1)$. The pseudomagnetic field inside the graphene crystal is given by

$$B_S = c\beta \frac{2\Phi_0 u_0}{a} = c\beta \frac{\Phi_0 \bar{u}}{aW} \quad (10)$$

where Φ_0 is the flux quantum. The effective magnetic length is $\ell_B = \sqrt{(aW)/(\beta \bar{u})}$. This field has the same dependence on the crystal dimensions and the maximum strain as in the examples discussed in Ref.24. For $W \approx 0.1$ micron and $\bar{u} \approx 10\%$ the generated effective field is of the order of 20T.

Experimentally, it may be difficult to create the precise stress distribution prescribed by Eq. (8). However, one can see that the required shape of the strained graphene crystal in Fig. 2 resembles an arc of a circle. To this end, we consider next the geometry in which a rectangular graphene crystal is bent into a circular arc, as sketched in Fig. 1 and shown in more detail in Fig. 3a. Note that this geometry is in fact standard for experimental studies of strain (see, e.g., Ref.8,10,11) with the only difference that the bending should be applied in plane rather than out of plane of a graphene sheet.

If the radius of the inner circle defining the lower edge in Fig. 3a is R, the shape of the deformed rectangle is given by

$$u_x(x,y) = (R+y)\sin\left[\frac{2x}{L}\arcsin\left(\frac{L}{2R}\right)\right] - x$$
$$u_y(x,y) = (R+y)\cos\left[\frac{2x}{L}\arcsin\left(\frac{L}{2R}\right)\right] - R - y \quad (11)$$

The undistorted rectangular shape is recovered for $L/R \to 0$. The displacements in Eq. (11) can be expanded in powers of R^{-1}, and the leading terms are

$$u_x(x,y) = \frac{xy}{R}$$
$$u_y(x,y) = -\frac{x^2}{2R} \quad (12)$$

These displacements do not exceed $\max(L,W)^2/R$. The next terms lead to corrections bound by $\max(L,W)^3/R^2$. The distortions in Eq. (12) coincide with those in eq. (9) in the limit of vanishing Poisson ratio $\lambda/(\lambda+2\mu) \to 0$ and lead to a uniform B_S inside the sample. The maximum strain is $L/2R$. For an arbitrary value of L/R, the pseudomagnetic field is given by

$$B_S(x,y) = -4c\frac{\beta\Phi_0}{aL}\arcsin\left(\frac{L}{2R}\right)\cos\left[\frac{2x}{L}\arcsin\left(\frac{L}{2R}\right)\right] \times$$
$$\times \left[1 - \frac{R+y}{L}\arcsin\left(\frac{L}{2R}\right)\right] \quad (13)$$

For $L/R \to 0$, the field reduces to $B_S \approx -c(\beta\Phi_0)/(aR)$, in agreement with Eq. (10) and the estimates given in Ref.24. The relative corrections to the constant value of B_S are of the order $L/2R$, that is, the maximum strain. An example of the field distribution described by Eq. (13) is plotted in Fig. 3b.

The found strain is not purely shear but it also contains a dilatation. The latter gives rise to an effective scalar potential[22], in addition to the discussed pseudomagnetic field. Below, we show that due to screening, the extra potential does not radically affect Landau quantization.

Following Ref.22, and using eqs. 9, this potential is:

$$V(x,y) = V_0\left(\partial_x u_x + \partial_y u_y\right) = V_0\left[2u_0 y + \frac{4\mu f_0}{f_1(\lambda+4\mu)}\right] \quad (14)$$
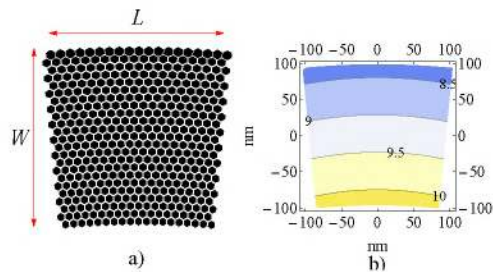

FIG. 3: (Color online). (**a**) - Rectangular graphene sample deformed into an arc. The radii of the lower and upper edges are R and $R+W$, respectively. The plot is for $R = 5 \times L$. (**b**) - Effective magnetic field, in Teslas, for the same deformed ribbon. Dimensions are $W = 200$nm, $L = 192$nm, $R = 5 \times L = 960$ nm. The maximum strain is 10%.
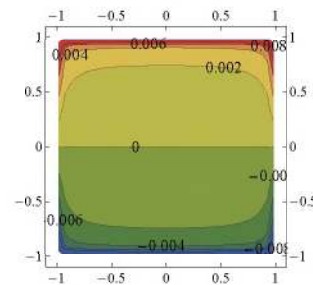

FIG. 4: (Color online). Variation in density, $\delta\bar{\rho}(\bar{x},\bar{y})$, in dimensionless units (see text) due to the screened scalar potential induced by strains. The aspect ratio is $L/W = 1$.

where $V_0 \approx 3$eV, estimated from the linear rise in the work function of graphene under compression between 0 and 10% strain[17] (note that in Ref.22 a much larger value of 16 eV is quoted, from old experimental data on transport properties of graphite). The constant contribution gives a rigid shift to all the levels while the non uniform term is equivalent to an effective electric field along the y direction. Unlike the strain induced gauge field, this potential will induce a charge redistribution and will be screened by the carriers in graphene.

We consider first the screening expected if we assume that the flake is a perfect metal, neglecting corrections due to quantum properties of the electron gas. The induced charge density, $\delta\rho(\vec{r})$ can be thus obtained from the condition

$$e^2 \int d^2\vec{r}' \frac{\delta\rho(\vec{r}')}{|\vec{r}-\vec{r}'|} = \frac{2V_0\bar{u}}{W}\delta\rho(\vec{r})y \quad (15)$$

This equation can be rescaled by the substitution $\delta\bar{\rho}(x/L, y/W) = (W+L)/(2L) \times (2V_0\bar{u})/(e^2 W) \times \delta\rho(x,y)$. where the function $\delta\bar{\rho}(\bar{x},\bar{y})$ depends only on the aspect ratio, W/L.

The density of carriers in a given Landau level due to the effective field given in Eq. 10, setting $c = 1$, is $\rho_{LL} = 2(aW)/(\beta\bar{u})$ so that $\delta\rho/\rho_{LL} = (W+L)/(2L) \times (4V_0 a)/(\beta e^2) \times \delta\bar{\rho}(x/L, y/W)$. Hence, the non uniform density induced by the effective field, in units of the

difference in densities between different quantum Hall plateaus, is approximately given by $\delta\bar{\rho}$ shown in Fig. 4.

To provide an ideal metallic screening, the chemical potential should coincide at each point with the positions of one of the Landau levels. Hence, the quantum energy of the carriers is larger than in a uniform electron distribution, when the Fermi energy lies in a pseudogap between the Landau levels. Thus, in addition to the classical screening energy, discussed above, we also must add the change in energy due to the changes in occupancies of the electron levels in the presence of the scalar potential. We first assume that the induced electronic density is given by the solution of Eq. 15, and that the electronic states are the Landau levels induced by the effective field in Eq. 10. Then, the two contributions to the energy, for $W \sim L$, are of the order:

$$E_{elec} \sim \frac{(V_0\bar{u})^2 L}{e^2}\langle|\delta\bar{\rho}|\rangle^2$$

$$E_{quantum} \sim \frac{v_F\beta V_0\bar{u}^2}{e^2}\langle|\delta\bar{\rho}|\rangle\sqrt{\frac{L}{a}} \qquad (16)$$

The calculations shown in Fig. 4 suggest that $\langle|\delta\bar{\rho}|\rangle = f \approx 10^{-2} - 10^{-1}$, and $v_F \sim e^2 \sim V_0 a$. Then, the scalar potential is screened, and the process can be described by the classical model outlined earlier, if $\sqrt{L/a} \gtrsim f^{-1}$, that is, $L \gtrsim 10^2 - 10^3$nm. For smaller sizes, the rigidity

of the quantum levels induced by the gauge potential prevents any rearrangement of the charge inside the flake. A detailed theory of screening in this situation will be presented elsewhere. In either case, the electronic states are well described by the effective Landau levels induced by the field in Eq. 10.

To create the required strain experimentally, one can think of depositing graphene ribbons onto a rectangular elastic substrate and deform it in the manner prescribed by eq. (9) or by bending it into a circular arc (Fig. 1). Crystals rigidly attached to the substrate can then be of arbitrary shape, as the strain distribution in the substrate would project onto graphene and give rise to a (nearly) uniform B_S. Note that macroscopic substrates would require the use of rubber-like materials capable of withstanding very large strains, such that local deformations projected on a submicron graphene crystals could still reach $\approx 10\%$.

[1] A. H. Castro Neto, F. Guinea, N. M. R. Peres, K. S. Novoselov, and A. K. Geim, Rev. Mod. Phys. **81**, 109 (2009).

[2] A. K. Geim, Science **324**, 1530 (2009).

[3] C. Lee, X. Wei, J. W. Kysar, and J. Hone, Science **321**, 385 (2008).

[4] T. J. Booth, P. Blake, R. R. Nair, D. Jiang, E. W. Hill, U. Bangert, A. Bleloch, M. Gass, K. S. Novoselov, M. I. Katsnelson, and A. K. Geim, Nano Lett. **8**, 2442 (2008).

[5] J. S. Bunch, S. S. Verbridge, J. S. Alden, A. M. van der Zande, J. M. Parpia, H. G. Craighead, and P. L. McEuen, Nano Lett. **8**, 2458 (2008).

[6] K. S. Kim, Y. Zhao, H. Jang, S. Y. Lee, J. M. Kim, K. S. Kim, J. H. Ahn, P. Kim, J.-Y. Choi, and B. H. Hong, Nature **457**, 706 (2009).

[7] M. L. Teague, A. P. Lai, J. Velasco, C. R. Hughes, A. D. Beyer, M. W. Bockrath, C. N. Lau, and N.-C. Yeh, Nano Lett. **9**, 2542 (2009).

[8] T. M. Mohiuddin, A. Lombardo, R. R. Nair, A. Bonetti, G. Savini, R. Jalil, N. Bonini, D. M. Basko, C. Galiotis, N. Marzari, K. S. Novoselov, A. K. Geim, and A. C. Ferrari, Phys. Rev. B **79**, 205433 (2009).

[9] W. Bao, F. Miao, Z. Chen, H. Zhang, W. Jang, C. Dames, and C. N. Lau, Nature Nanotechnology **4**, 562 (2009).

[10] M. Huang, H. Yan, C. Chen, D. Song, T. F. Heinz, and J. Hone, Proc. Nat. Ac. Sci. (USA) **106**, 7304 (2009).

[11] G. Tsoukleri, J. Parthenios, K. Papagelis, R. Jalil, A. C. Ferrari, A. K. Geim, K. S. Novoselov, and C. Galiotis, Small (2009), DOI: 10.1002/smll.200900802.

[12] V. M. Pereira, A. H. C. Neto, and N. M. Peres, Phys. Rev. B **80**, 045401 (2009).

[13] P. L. de Andrés and J. A. Vergés, Appl. Phys. Lett. **93**, 171915 (2008).

[14] M. M. Fogler, F. Guinea, and M. I. Katsnelson, Phys. Rev. Lett. **101**, 226804 (2008).

[15] V. M. Pereira and A. H. Castro Neto, Phys. Rev. Lett. **103**, 046801 (2009).

[16] D. W. Boukhvalov and M. I. Katsnelson, J. Phys. Chem. C **113**, 14176 (2009).

[17] S.-M. Choi, S.-H. Jhi, and Y.-W. Son (2009), arXiv:0908.0977.

[18] J. Viana-Gomes, V. M. Pereira, and N. M. Peres (2009), arXiv:0909.4799.

[19] M. Mohr, K. Papagelis, J. Maultzsch, and C. Thomsen (2009), arXiv:0908.0895.

[20] R. M. Ribeiro, V. M. Pereira, N. M. Peres, P. R. Briddon, and A. H. Castro Neto (2009), arXiv:0905.1573.

[21] M. Farjam and H. Rafii-Tabar (2009), arXiv:0909.5052.

[22] H. Suzuura and T. Ando, Phys. Rev. B **65**, 235412 (2002).

[23] J. L. Mañes, Phys. Rev. B **76**, 045430 (2007).

[24] F. Guinea, M. I. Katsnelson, and A. K. Geim (2009), Nature Physics, DOI:10.1038/NPHYS1420.

[25] L. D. Landau and E. M. Lifschitz, *Theory of Elasticity* (Pergamon Press, Oxford, 1959).

[26] K. V. Zakharchenko, M. I. Katsnelson, and A. Fasolino, Phys. Rev. Lett. **102**, 046808 (2009).